Rev.Adv.Mater.Sci. 5 (2003) 166-170

STRUCTURAL ORDERING OF METAL-CONTAINING AMORPHOUS CARBON THIN FILMS INDUCED BY LOW-ENERGY ELECTRON BEAM PROJECTION

Eiji Iwamura

PRESTO, Japan Science and Technology Agency, RCAST, The University of Tokyo, 4-6-1 Komaba, Meguro-ku, Tokyo 153-8904, Japan

Received: July 05, 2003

Abstract. Localized graphitization and structural ordering in sputter-deposited amorphous carbon films with a small amount of cobalt and rhodium were investigated using transmission electron microscopy, low-energy electron energy-loss spectroscopy and temperature dependent conductivity measurement. Electrons accelerated with 60 kV were irradiated to 100 nm-thick a-C films deposited on Si substrates through a 3-micron-thick Si window. As the result of the electron beam projection, two steps of graphitization occurred at relatively low process temperature in the 15at.%Co:a-C films. The first one was strongly related to the presence of Co. Spherical graphitic shells formed at the interface of fcc-Co grains following shrinkage of the encapsulated crystals. The second one was independent of the Co catalyst. Large plate-like graphitic structures formed in the region where Co atoms became absent as the result of agglomeration. In the 1at.%Rh:a-C films, short range structural ordering with formation of graphitic phases was observed and significant change in conductivity mechanism was detected in the temperature range from 15K to RT.

1. INTRODUCTION

Carbon-based materials have been regarded as one of the most important material in nanotechnology. Not only nanotubes and fullerenes, but also a noble form of nanocomposite carbon structures consisting of amorphous carbon with fullerene-like inclusions has recently attracted extensive interests [1]. Various synthesis techniques, such as cathodic arc deposition [2], ion-implantation [3], co-vaporization of cobalt and C_{60} [4] and FIB-CVD/annealing [5], have been reported, however, the way to control functionally hybridized order/disorder structures has not been established yet.

In this study, a new technique using low-energy electron beam (EB) irradiation was investigated to form ordered/disordered composite structures in amorphous carbon thin films. Amorphous carbon thin films containing a small amount of metal elements (Me:a-C) exposed to an electron shower of which the energy and dose rate were much smaller compared to an intense electron beam in an electron microscopy. Two cases of localized ordering were examined. One was the graphitization in Co:a-C films which contained onion-like structures and plate-like graphitic structures. The other was short range structural ordering in Rh:a-C films which affected electrical conductivity.

2. EXPERIMENTAL PROCEDURE

2.1. Film preparation and characterization

Metal-containing amorphous carbon films having a thickness of 100 nm were deposited onto 4-inches Si (100) substrates by dc magnetron sputtering in a $2.0 \cdot 10^{-1}$ Pa argon atmosphere. Using a mosaic tar-

Corresponding author: Eiji Iwamura, e-mail: iwamura@odin.hpm.rcast.u-tokyo.ac.jp

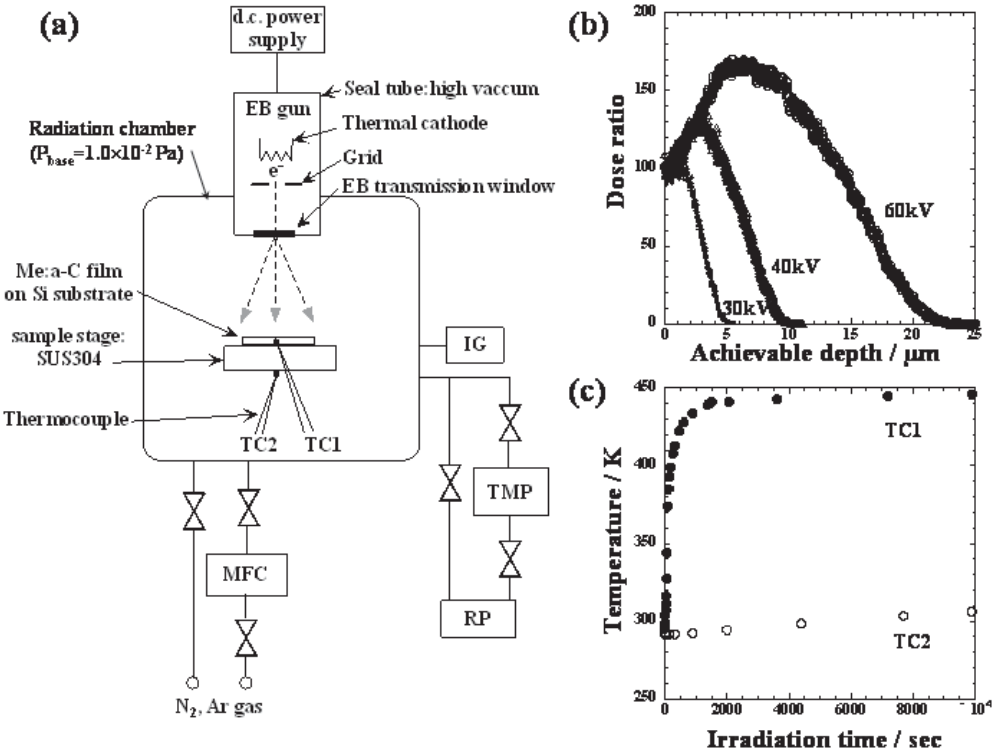

Fig. 1. (a) Schematic diagram of electron beam radiation system. (b) Achievable depth of electrons in Si wafer after transmitting a 3 μm Si window as a function of accelerating voltage. (c) Temperature induced by electron irradiation accelerated by 60 kV as a function of irradiation time.

get arranging several 5×5mm metal chips on an anisotropic graphite target, content of metal elements was varied by changing the numbers and/or the position of the metal chips on the graphite target. Two types of alloying element were examined. One is Co with 15 at.%, which is known as a catalyst for graphitization and tended to be easily aggregated in amorphous carbon matrix. The other is Rh with 1 at.%, which was finely dispersed in the films even after electron beam irradiation. Composition of the films was measured by induction coupled plasma analysis and Ruterford backscattering. The substrate was water cooled during deposition. The sputtering dc power density was 0.057 W·mm^{-2}, and the resultant deposition rate was in the range from 0.5 to 0.7 nm·sec^{-1}. Subsequently, the films were exposed to an electron shower using a low-energy electron beam radiation system (Min-EB manufactured by USHIO Inc). The details of the process are described in the following section. Plan-view and cross-sectional microstructures were characterized by a transmission electron microscopy (HF-2000, HITACHI) operating at 200 kV and electron energy loss spectra which were acquired in the energy range up to 38 eV. Electrical conductivities were measured in the temperature range between 15K and 300K by four point probe method in a vacuum less than 1.0·10^{-3} Pa.

2.2. Low-energy electron beam irradiation

Fig. 1a shows the schematic diagram of the low-energy electron beam radiation system. The electron emission unit consisting of a thermal cathode and a grid was encapsulated into a glass tube sealed in a high vacuum. Electrons from the hot cathode were accelerated by the potential difference between the cathode and the electron beam transmission window and emitted into the radiation chamber. The accelerating voltage and current was 60 kV and 0.3 mA respectively. The window was made of a 3 μm Si film. As electrons passed though the window, energy was reduced and the electron beam was scattered. The Me:a-C film specimen diced into the size of 10×10 mm were placed on the stage and exposed to the electron shower. The gap between the window and the specimen was set in 15 mm. The electron dose showed linear relation to the ac-

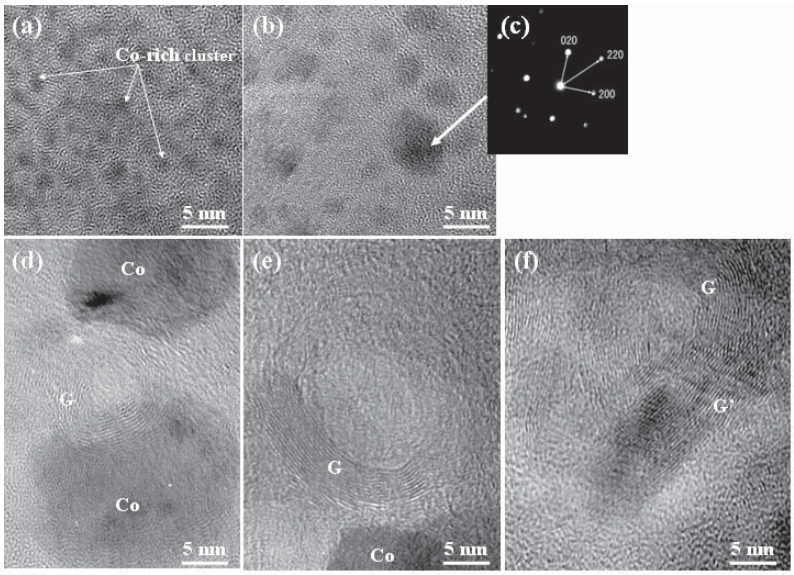

Fig. 2. TEM micrograph series showing evolution of graphite-like structures by electron beam projection accelerated by 60 kV: (a) as-deposited, (b) EB irradiation for 1.8 ksec, (d) EB irradiation for 3.6 ksec, (e) EB irradiation for 9.9 ksec and (f) EB irradiation for 19.8 ksec. (c) Electron diffraction pattern obtained from the gray phase indicated with an arrow.

celerating voltage and the gap, and dose rate was 3.1 $\mu C \cdot sec^{-1} \cdot cm^{-2}$ in the conditions used in this study. The operating chamber pressure was about $1.0 \cdot 10^{-2}$ Pa and remained constant during the irradiation process.

Transmission depth and energy absorption rate are generally determined by the electron energy, which is attributed to accelerating voltage, and material density. The electron path can be approximated by the following equation [6]:

$$S = 0.0667 V^{5/3}/\rho,$$

where S is electron path vertical to material surface, V is accelerating voltage and ρ is mass density in which the electrons transmit. Fig. 1b shows an achievable depth profile in a Si wafer of electrons estimated by Monte Carlo simulation. Assuming that the electrons are accelerated by 60 kV, after transmitting through the Si window, most of their energy is lost within about 10 μm from the top surface and the maximum achievable distance is about 20 μm at most. Thus high energy can be efficiently applied to a thin layer of the sample surface without increasing temperature of the whole system. Fig. 1c shows the change of temperature of the specimen and stage during electron beam projection. Thermo couples were weld to a specimen about 50 μm underneath the film surface (TC1) and to the sample stage (TC2). The specimen temperature quickly increased as the electron beam irradiation started, and saturated at about 450K in 2 ksec. The temperature of the sample stage gradually increased up to about 310K during the irradiation. Therefore, it is possible to keep specimen and system in relatively low temperature in this process.

3. RESULTS AND DISCUSSION

3.1. Graphitization behavior of 15at.%Co:a-C films

Figs. 2a-2f are plan-view TEM micrographs of the 15at.%Co:a-C showing microstructural change induced by the electron beam irradiation. Fig. 2a is the as-deposited film showing Co-rich amorphous clusters with about 1 nm in size uniformly dispersed in the a-C matrix. Fig. 2b was obtained from the film which was irradiated for 1.8 ksec. As EB irradiation started, the Co-rich clusters started to coalesce and crystallization of Co was occurred subsequent to reaching a certain size. The nano-beam electron diffraction pattern as shown in Fig. 2c indicated that the amorphous Co-rich cluster crystallized to form fcc-Co. On the early stage of EB irradiation, structural ordering of the a-C matrix was indistinctive. Fig. 2d and 2e were the microstructures after EB irradiation for 3.6 ksec and 9.9 ksec , respectively.

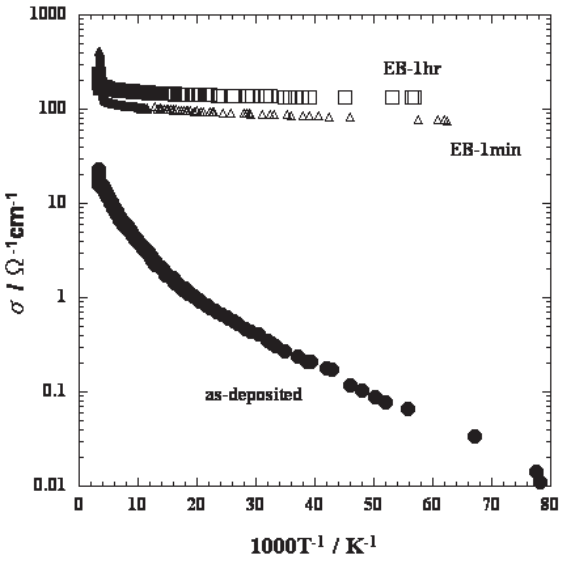

Fig. 3. Electrical conductivity as a function of the inverse temperature of 1at.%Rh:a-C films before and after the low-energy EB irradiation.

Grain growth of the fcc-Co was progressed and layered shell structures with spacing of graphite c-plane were frequently formed in the a-C matrix. The size of the shell structures and a number of stacks of graphitic layers were increased as the irradiation time increased. The surrounding area of the ordered carbon structures found to remain amorphous, while there appeared to be fragments of graphitic structures. Most of the shell structures had a-C in the core, and only a few had a fcc-Co core. No evidence of carbide or solid solution of carbon in the Co grains was obtained. With further irradiation as shown in Fig. 2f, a different type of graphitic structures (indicated by the letter G') were observed in addition to fragments of the shell structures. The graphitic structure appeared not to be distorted but plate-like, and the maximum size reached about 15 nm in width and about 30 nm in length, much larger than the size of the Co grains.

The shell structures and plate-like structures were observed in the corresponding cross-sectional microstructures as well. Therefore the layered shell structure corresponds to onion-like morphology. It is presumed that the graphitization process consists of two steps.

The first one is strongly related to the presence of Co as a catalyst. The graphitization behavior in contact with Co observed in situ in TEM was precisely reported in the literature [7-10]. The appearance of the onion-like structures implied that the graphitization process was similar to that observed by Banhart in which spherical graphitic shells form at the interface of Co grains following shrinkage of the encapsulated crystals. The grain growth of Co was considered to bring about by Ostwald ripening and coupled with the graphitization of the surrounding a-C matrix. The variation of grain size d with EB irradiation time t was $d \propto t^{1/2}$. This dependence indicates that the grain growth is governed by interface reaction. As Co atoms and clusters migrate outward through the shell structure [9], the permeability of the onion-like structures presumably dominates the process.

The second graphitization seems to be independent to the Co catalyst. Concurrently with the grain growth, cobalt diffused toward the surface and eventually agglomerated in the vicinity of the film surface. As a result, large areas where Co became absent were formed in the films and the plate-like graphitic structures appeared to form in the region. Since the plate-like structures formed in the area where carbon did not contact the Co grains anymore and the size was far larger than that of the fcc-Co grains, the formation mechanisms is different from that of the onion-like structures. The second graphitization appeared to be significant rearrangement of carbon network in the film independent of Co grains.

3.2. Change of electrical conductivity of 1at.%Rh:a-C films

In contrast with significant aggregation of Co in a-C matrix during the EB irradiation process, rhodium dispersed finely in the films and the graphitization as shown in the Co:a-C film was not observed. In high resolution TEM micrographs, it was hard to identify structural change induced by the EB irradiation. However, electron energy loss spectrum revealed a increase of π bonding in the amorphous matrix by a broad plasmon-loss peak observed in the range between 4 eV and 8 eV. The fact is indicative of short range structural ordering with formation of graphitic phases. Moreover, significant change in conductivity mechanism which can be attributed to the structural ordering was detected in the temperature range from 15K to RT. Fig. 3 shows the dependence of electrical conductivity on temperature in 1at.%Rh:a-C films before and after the EB. At temperatures below 250K, the conductivity of the irradiated film, even for 60 sec irradiation, showed a weak dependence on temperature while significant temperature dependence of conductivity

was observed in the as-deposited film. At above 250K, activation energy for thermal excitation process of carriers became 1/3 of that of the as-deposited film as a result of the EB irradiation. The conduction mechanisms in amorphous carbon films are closely related with the film microstructure and the C-C bonding [11]. The structural ordering presumably affect localized state at the Fermi level or carrier density in the structure, although further detailed studies are necessary to clarify the conduction mechanisms of the metal including amorphous carbon films.

4. SUMMARY

Sputter-deposited amorphous carbon thin films containing 15 at.%Co and 1 at.%Rh were exposed to an low-energy electron shower, and localized graphitization and structural ordering were investigated. The following results were obtained.

1. Structural ordering of the metal-containing amorphous carbon films occurred at relatively low process temperature range, which was up to 473K in the specimen and less than 310K in the sample stage, using the low-energy electron beam projection.
2. In the 15at.%Co:a-C films, two steps of graphitization behavior was observed. The first one was strongly related to the presence of Co. Spherical graphitic shells formed at the interface of fcc-Co grains following shrinkage of the encapsulated crystals. The second one was independent to the Co catalyst. Large plate-like graphitic structures formed in the region where Co atoms became absent as the result of agglomeration.
3. In the 1at.%Rh:a-C films, electron energy loss spectrum revealed short range structural ordering with formation of graphitic phases. In addition, significant change in conductivity mechanism was observed in the temperature range from 15K to RT.

ACKNOWLEDGEMENTS

The author would like to thank Mr. Masanori Yamaguchi of Ushio Inc. for his help in characterization of electron beam irradiation process. Thanks are also due to Mr. Kiyoshi Yamamoto of Kobelco Research Institute, Inc., for TEM works.

REFERENCES

[1] H.Sjostrom, S. Stafstrom, M. Boman and J.-E. Sundgren // *Phys. Rev. Lett.* **75** (1995) 1336.
[2] G.A.J. Amaratunga M. Chhowalla, C.J. Kiely, I. Alexandrou, R. Ahrronov and R.M. Devenish // *Nature* **383** (1996) 321.
[3] E. Thune, T. Cabioc'h, Ph. Guerin, M.-F. Denanot and M. Jaouen // *Materials Letters* **54** (2002) 222.
[4] V. Lavrentiev, H. Abe, S. Yamamoto, H. Naramoto and K. Narumi // *Physica B* **323** (2002) 303.
[5] J. Fujita, M. Ishida, T. Ichihashi, Y. Ochiai, T. Kaito and S. Matsui // *J.Vac.Sci.Technol.* **B20** (2002) 2686.
[6] S. Schiller, *Electron Beam Technology* (John Wiley & Sons, 1983).
[7] T.J. Konno and R. Sinclair // *Acta. Metall. Mater.* **43** (1995) 471.
[8] A.G. Ramirez, T. Itoh and R. Sinclair // *J. Appl. Phys.* **85** (1999) 1508.
[9] F. Banhart, N. Grobert, M. Terrones, J.-C. Charlier and P.M. Ajayan // *International J. Modern Physics B* **15** (2001) 4037.
[10] F. Banhart, Ph. Redlich and P.M. Ajayan // *Chem. Phys. Lett.* **292** (1998) 554.
[11] C.A. Dimitriadis, N.A. Hastas, N. Vouroutzis, S. Logothetidis and Y. Panayiotatos // *J. Appl. Phys.* **89** (2001) 7954.